MECHANOTRANSDUCTION

IN THE DEVELOPING

MURINE PROSTATE

by

Elizabeth Marcin

A thesis submitted to the Faculty of the University of Delaware in partial fulfillment of the requirements for the degree of Honors Bachelor of Science in Neuroscience with Distinction

Spring 2019

MECHANOTRANSDUCTION

IN THE DEVELOPING

MURINE PROSTATE

by

Elizabeth Marcin

Approved: _____

Jason Gleghorn, PhD
Professor in charge of thesis on behalf of the Advisory Committee

Approved: _____

Gary Laverty, PhD
Committee member from the Department of Biological Sciences

Approved: _____

Carlton Cooper, PhD
Committee member from the Board of Senior Thesis Readers

Approved: _____

Earl Lee II, Ph.D.
Deputy Faculty Director, University Honors Program

ACKNOWLEDGMENTS

I would like to thank everyone in the Gleghorn lab for their continuous support and patience over the last four years. Their never-ending support, positivity, and selfless dedication to science has not only facilitated the progression of this project but has shaped me into the student and scientist I am today. I would like to specifically thank Dr. Gleghorn for his patient supervision, giving me the autonomy to fail and learn in lab; and I would also thank Dr. Joshua Morgan for his personal and profession guidance early in my time at the lab and his efforts in the initiation of the project. A special thanks to Rachel Gilbert, a graduate student in the lab, who tirelessly helped me work through the molecular mechanisms, hypotheses, techniques, and designs involved in the project over the years. I would like to show my appreciation to my other committee members, Dr. Carlton Cooper and Dr. Gary Laverty for their input and assistance in developing my thesis

Additionally, I would like to thank the Undergraduate Research program for their funding through supply and expense grants as well as summer scholars funding. Finally, I would like to thank my family and friends, specifically Laurel Schappell, for always being there as a sounding board, a support system, and an outlet. Everyone here has played an integral role in both my personal and professional growth throughout college, and this project could not have been completed with them.

TABLE OF CONTENTS

LIST OF TABLES

LIST OF FIGURES

ABSTRACT

Prostate cancer and benign prostate hyperplasia (BPH) are two of the most common diseases affecting men - with 50% of middle-aged men suffering from BPH and 12% of men diagnosed with prostate cancer in their lifetime. Both pathologies involve dysregulated epithelial growth and structural abnormalities that influence the mechanical forces experience within the prostate lumen. As the role some smooth muscle contraction and mechanically sensitive ion channels are elucidated in both the developing and adult prostate, compounding evidence suggests that changes in mechanical forces experienced by the epithelial cells both pathologically and in development could influence epithelial phenotype and abnormal growth evident in BPH and cancer. To understand the type and impact of these forces on benign and malignant growth, it is pertinent to understand the impact of mechanical forces on normal/regulated epithelial growth during development. To study this, a 3D model with high physiological relevance is needed. Therefore, the first aim of this project is to develop successful 3D culture models that allows one to alter various mechanical forces both intraluminally and externally of the prostate. The second aim entails using such a model to determine whether fluid induced forces influence prostatic cell differentiation, expression, and phenotype in respect to the general morphology in development. The results suggest that the morphology and epithelial growth rate of the prostate does change in response to intralumenal pressure and environmental density. The models and preliminary data documented in this project are a critical step towards a comprehensive understanding of the role of mechanical forces in prostate disease

Chapter 1

INTRODUCTION

1.1 Benign Prostate Hyperplasia

Nearly 50% of men suffer from Benign Prostate Hyperplasia (BPH) once they reach the age of fifty and it is the most common cause of lower urinary tract symptoms[1]. Men suffering from BPH often experience incontinence, trouble urinating, and pain while urinating. The cause of BPH remains unknown, though more recently a variety of factors such as diet, lifestyle, inflammation, and hormonal variations have been linked to BPH development and progression[2,3]. Additionally, though BPH has not been directly named as a precursor to prostate cancer, it is often associated with increased risk of prostate cancer[2].

1.2 Prostate Cancer

Prostate cancer is the second most common type of cancer in men and affects nearly 12% of men. This means in the US alone, there are 174, 650 new cases per year[1]. If caught early, it is treatable with surgery; without treatment, however, it easily metastasizes to the bone, often leading to death. Diagnosis of prostate cancer usually requires a biopsy for a histological stain to determine cell phenotype.

1.3 Pathophysiology of Prostate Cancer and BPH

The Pathophysiology of Prostate Caner and BPH is complex, with alterations of inter and intramolecular signaling pathways, changes in ECM expression, and overall morphological abnormalities.

1.3.1 Histology of Prostate Cancer and BPH

Both prostate cancer and BPH involve luminal maldevelopment. Clinical studies examining biopsies from patients with BPH have found abnormal epithelial histology in which small blockages in distal luminal buds exhibit increased epithelial growth and morphological irregularities downstream of the blockage. Similar abnormalities occur to a more sever degree in prostate cancer, described as clear prostatic intraepithelial neoplasia (PIN) structures. As the severity of these PIN structures increases, the epithelial cells proliferate in an uncontrolled manner with less defined cell structure and organization while the surrounding mesenchyme and luminal space diminish[4]. This degree of disorganization and epithelial proliferation increases with the severity of the disease.[3]

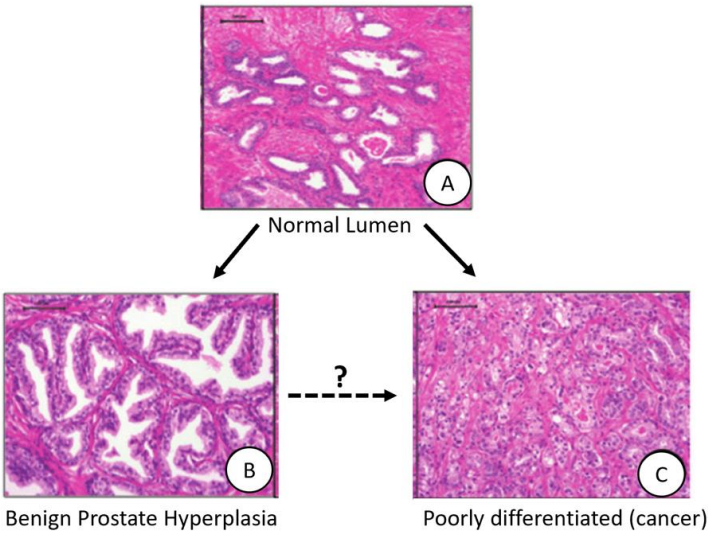

Figure 1; Histological sample A depicts a normal histological stain of prostate lumen, compared to B, which depicts a histological sample from BPH, and C, a stained prostate cancer sample showing the severe PIN structure characterized by luminal proliferation and disorganization. This is comparable to sample B in which epithelial proliferation is present yet maintains epithelial organization. (Oncology letters, 2014).

1.3.2 Mechanotransduction in Abnormal Prostate Epithelium

Epithelial dysregulation is a major factor in cancer progression and metastasis, and phenotype switching of epithelial cells is common among most cancers[13]. In prostatic cancer cell lines, it has been shown that mechanotransduction based on the stiffness of the culture environment influences the ability of the cancer cells to shift towards epithelial-mesenchymal transition (EMT) or the opposite, mesenchymal to epithelial transition (MET). Cells undergoing EMT are more likely to exhibit metastatic qualities whereas cells going through MET are more likely to form lesion-like structures[5,6]. Interestingly, under stiffer culture conditions, prostate cancer cell lines shift towards EMT and are prevented from shifting to MET upon chemical

stimulation[5]. Literature also supports the theory that interstitial hypotension promotes EMT[6,7].

1.4 Fluid-Induced Forces in the Prostate

The prostate develops in buds protruding into the surrounding mesenchymal tissue from breaks in the smooth muscle that lines the already developed urethra. These buds grow to form branch-like structures of lumen that become more complex and intertwined distally. As the lumen grow, the epithelium interacts with the mesenchyme, inducing smooth muscle differentiation of the mesenchyme, creating a lining of contractile smooth muscle around the epithelial layer[8,9]. In development, the smooth muscle contracts sporadically, pushing fluid through the lumen, creating fluid-induced forces along the newly differentiating epithelium[8,10]. In the adult prostate, smooth muscle contracts to push prostate fluid created in the distal glands towards the more proximal lumen to prepare for use[11]. Then, during ejaculation, the entire prostate contracts in synchrony, pushing the prostate fluid into the urethra to facilitate sperm motility.

It has been well established in development that fluid-induced forces provide a means of morphogenic regulation via cell polarization and signal transduction induced through mechanically active ion channels (MAICs). A variety of MIACs have been identified in the prostate epithelium such as Transient Receptor Potential Cation Channels (TRPs)[12,13,14], and the Cystic fibrosis transmembrane conductance regulator (CFTR)[15]. These channels play critical roles in shaping development of other tissues in response to mechanical forces, therefore, it is increasingly likely that fluid-induced forces play a role in prostate development and prostate epithelial differentiation. Additionally, TRPV6 and TRPM8, two subfamily TRP channels, have been identified

in the prostate cancer cell line (LNCaP) as regulators of store-operated Calcium channels[16,17,18]. Because Calcium plays such a central role in regulating cell metabolism, gene expression, and signaling pathways – especially extracellular ATP release[19,20] – it's likely that these MAICs influence mobility and extracellular communication of adult epithelial cells[21].

Clinical studies implicate the role of hydrostatic pressure in BPH as well. With age, the internal spermatic vein integrity degrades, increasing pressure and causing retrograde flow and subsequent venous accumulation into the prostate drainage system and prostate. As a result of both the engorged vein and leakage leading to increased interstitial fluid, the hydrostatic pressure and free testosterone are increased – theoretically leading to hypertrophy and hyperplasia, respectively, quintessential aspects of BPH. Though not discussed in this paper, testosterone is a known to induce growth factor expression and epithelial growth in both prostate development and in cancer cells. Once the vein is surgically drained, the BPH patients in the study experienced symptom relief and a decrease in prostate volume[22].

Additionally, it has been hypothesized that blockages in the adult prostate, possibly a cluster of epithelial cells, can occur in the distal tips of the lumen, and as the surrounding smooth muscle contracts, it creates an increase in intraluminal pressure[23,29]. The pressure in the blocked lumen increases over time, possibly altering the phenotype of the lodged epithelial cells in the cluster to a dedifferentiated state in which more growth factors are expressed and the cell proliferation is less regulated[24]. Then, it can be suddenly dislodged and pushed with the prostatic fluid to a different part of the prostate where it can proliferate and initiate the formation of PIN structures.

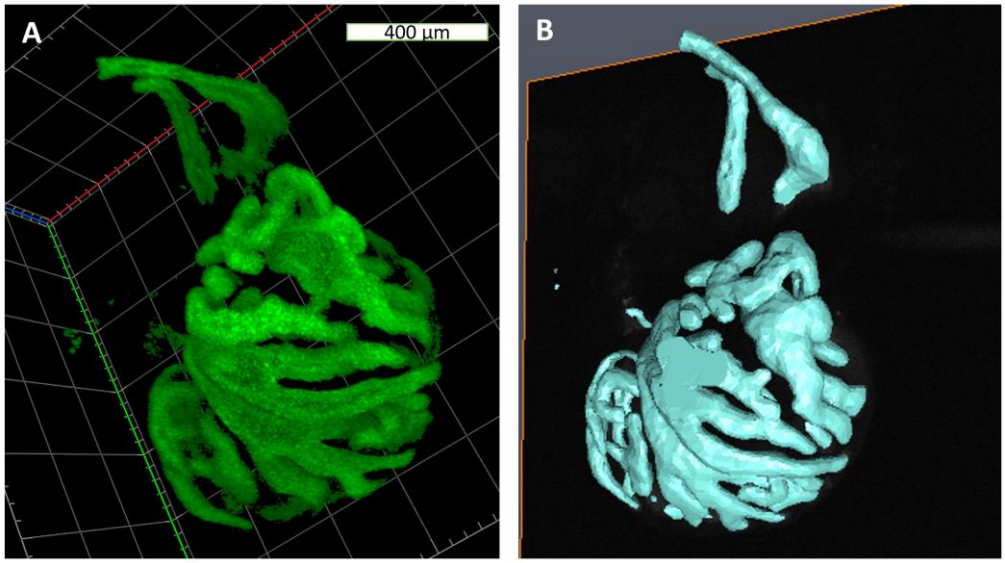

Figure 2; A) a dissected p7 murine prostate ventral lobe stained by immunofluorescence for E-Cadherin (green)to show luminal structure and branching early in prostate development. B) a 3D model created in Amira to clarify branching junctions and calculate total volume of the lumen.

1.5 Current Studies and Models

Understanding the impact of mechanical forces in the normal growth of development could be applied to understanding the role of these forces in benign and malignant growth in the adult prostate. The majority of research prostate research, however, is focused on strictly biological signaling pathways and gene expression, leaving a relatively large gap in literature discussing mechanical forces and mechanotransduction within the prostate, especially the developing prostate. Important pathway activation and signal cascades have been identified in prostate development, but no information exists on the role of smooth muscle contractions and fluid-induced forces during early prostate differentiation and development.

Most studies of the prostate are specifically geared toward prostate cancer metastasis and progression, in that they use either immortalized prostate epithelial cancer cell lines in experiments or take a more clinical approach studying histological biopsies of tumors and relevant comorbidities of patients presenting varying stages of cancer. Using these already immortalized cell lines presents the uncontrollable and incompletely documented variable of altered gene expression and subsequent phenotype intrinsic to a cancerous cell[25,26]. Some more recent studies have used primary epithelial cell lines[27,28], however, these studies are still mostly conducted in 2D in a tissue culture dish, eliminating the complexity of 3D environmental interactions and complex microenvironment fluid movements.

With increasing popularity of 3D models, studies have been done using prostate acini, however, often these acini are often created using a cancer cell line. Notably, primary cell acini have been achieved, and look like a promising tool to study epithelial-epithelial special interactions[18,30,]. Unfortunately, however, primary cells are time consuming to separate, and it is difficult to passage acini cultured in a gelatinous suspension. Another interesting study took an alternative approach to 2D culture and grew prostate cancer cells on a membrane then used in Ussing Chamber experiments to determine how hyper/hypoosmotic pressure applied to the basal/apical sides of the epithelial cells effects the cellular release of ATP[19]. This study is one of the first implicating pressure and external forces directly to intercellular communication pathways between cancerous prostate epithelial cells. Though creative, these studies still only focused on single cell lines rather than interactive tissues.

Though these single cell line models allow for specific data with fewer confounding variables, they do not accurately represent the complex interactions between various tissue and cell types found in nature. There is significant literature describing the constant balance maintained between the epithelium, stroma, and mesenchyme to regulate cell differentiation, organization, and function during prostate luminal development[7]. The body is so effective at maintaining homeostasis, that often tissues compensate for specifically inhibited pathways or exhibit unexpected compound reactions to a stimulus. These synergistic functions and feedback loops between tissues make a multicellular if not full explant model significantly more physiologically relevant than traditional cell line experiments.

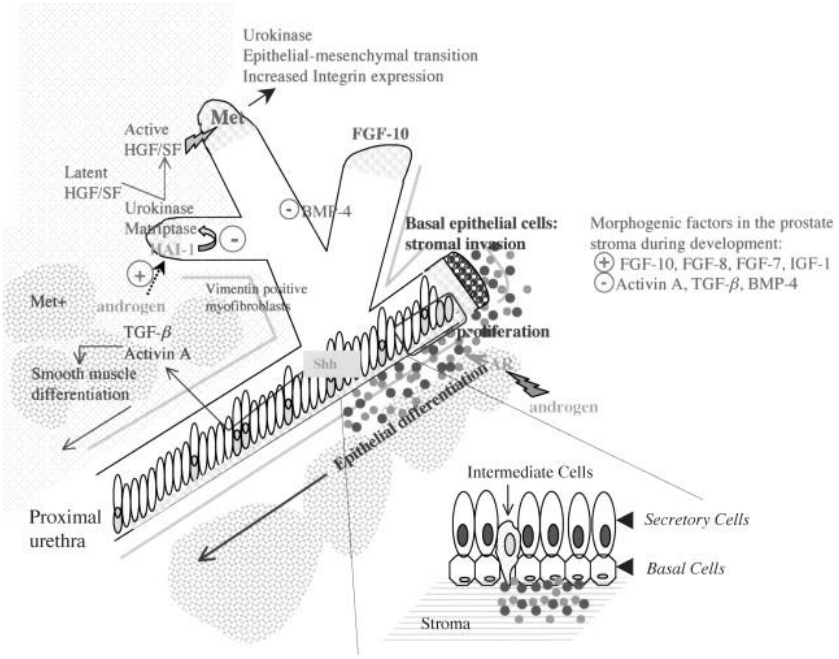

Figure 3; Major growth factors and proteins involved in differentiation and formation of the epithelium, stroma, and mesenchyme of the developing prostate lumen. (Stem Cell Reports, 2016)

1.6 Hypothesis and Specific Aims

I hypothesize that fluid-induced forces play a role in regulating epithelial phenotype and proliferation in prostate development and the progression of adult prostate pathologies. Therefore, a specific aim of this project is to develop a successful 3D culture model that allows one to alter various mechanical forces both intraluminally and externally of the prostate to determine the effect on cell proliferation, differentiation, and over-all organ morphology.

First, I plan to determine whether fluid-induced forces influence murine ventral lobe growth and development. Understanding how fluid forces influence specific cell differentiation, expression, and phenotype in respect to the general morphology of the organ provides an exciting starting point for subsequent research determining the molecular signaling pathways involved in these mechanically reactive tissues. These molecular changes induced by fluid forces in development can likely be applied to understanding the causation of BPH and progression of prostate cancer so both pathologies can be deterred in the future.

1.6.1 Proposed Model

The proposed model is an explant model to create a system as physiologically relevant as possible. This entails maintaining access to nutrients within the explant, continual hydration of the organ, and physiological culture conditions. Additionally, the explant would allow for study of different cell types of interest, such as epithelium, stromal myofibroblasts, and mesenchyme to maintain junctions and interact as they would *in vivo*. The integrity of the luminal structure within the mesenchyme would be maintained as well, allowing for orientation and identification relative expression patterns during the imaging process. More specifically, the explant model needs to be

able to be imaged using either epifluorescent or confocal microscopy, therefore the tissue itself would not exceed a thickness of 500 um.

Additionally, a device used for explant culture would facilitate the experimenter's ability to increase or decrease external hydrostatic pressure, manipulate intralumenal pressure, and manipulate external environment properties like stiffness. Simultaneously, the system would not impose uneven, non-physiological stresses on the explant, such as those that would be experienced by pressing the explant against a hard surface or stiff membrane.

Chapter 2

METHODS

2.1 Whole Organ Explant Model

The first system used was whole dissection of the postnatal murine reproductive system, as well as the bladder, with the urethra sutured shut to provide a "closed" biological system. The explant was placed prone on a membrane, suspended over explant media (DMEM F12 media with 5% Fetal Bovine Serum) and cultured for 24-48 hours in an incubator. An "open" system was created by leaving the urethra unsutured, therefore preventing the organs from building up fluid pressure. Tissue fixtation, antibody staining and epiflourescent microscopy was used to analyze the explants after culture.

2.1.1 Dissection Technique

Wild type CD1 mice were bred and raised in accordance with University of Delaware IACUC protocols until the desired point of neonatal development of p7. Upon reaching the appropriate gestational age, mouse pups were euthanized via peritoneal injection of 250mg/kg of sodium pentobarbital into the lower right quadrant of the abdomen, above the pelvis. Upon confirmation of death by lack of reflexive response, the mouse was sprayed with 70% ethanol and placed prone on a petri dish. Small dissecting scissors were used dislocate and break both hips, allowing for easier access to the lower abdominal cavity. A medial incision piercing the peritoneum was made parallel to table between the anus and the tail of the mouse. The incision is continued to the left and right along the peripheral edges of the lower abdominal cavity. The skin and peritoneum can then be folded upwards and cut away, exposing the stomach, colon, liver, and bladder. Using forceps to lift the bladder, the exposed

ureters and descending colon were cut. Turning the scissors horizontally, and starting at the initial incision site, a medial cut was made along the spine for 2-4cm with careful consideration to angle the scissors down to prevent damage to the dorsal prostate or urethra. Once the organ system was freed, it was placed in a petri dish of PBS in which excess connective tissue, fat, and blood could be removed under light microscopes. The bladder was sutured off at the neck and the testes were were sutured off at the vas deferens to prevent variable testosterone, so the final explant consisted of the seminal vesicles, all lobes of the prostate, and the urethra.

2.1.2 Membrane Suspended Device Construction

20 grams of polydimethylsiloxane (PDMS) was mixed in a 90mm Petri dish and desiccated until all air bubbles were expunged. The PDMS was then baked at 60^{o}C overnight to polymerize at 2mm thickness. The PDMS was cut into 1cm by 3cm rectangles and sprayed with 70% ethanol for sterilization purposes. Once dry, two blocks were placed about 1.5cm apart in a sterile 6 well tissue culture dish. An opaque micropore membrane was halved and placed down longways, bridging the two PDMS blocks. 400uL of explant media was pipetted under the membrane and the organ explant was placed prone onto the membrane. A 200uL droplet was pipetted on top of the explant. This was repeated for all explants. About 3 mL of sterile water filled the inter-well space to mitigate media evaporation over the incubation period.

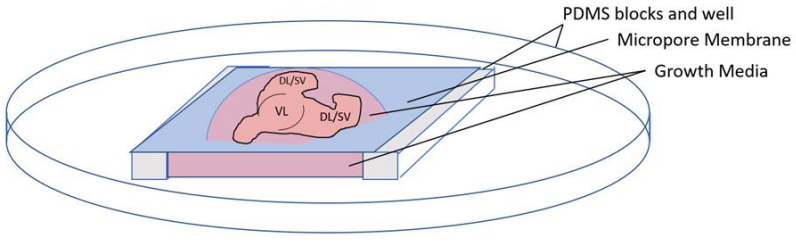

Figure 4; Diagram depicting a membrane suspension device described above.

2.1.3 Staining and Microscopy

Whole explant samples were fixed in 4% paraformaldehyde (PFA) overnight on a benchtop rocker at 4ºC. They were then permeabilied using 0.05% Triton-X100 solution overnight at 4ºC. Unlike the whole samples, single lobe samples were fixed in 4% PFA for 45 minutes at room temperature and were permeabilized with 0.05% Triton for 1 hour at room temperature. Following fixation, all samples were triple washed with 1x phosphate-buffered saline (PBS), and placed in blocking buffer overnight at 4ºC on a rocker. For proliferation assays, a Click-it EdU Alexa Fluor kit by Thermo Fisher was implemented prior to antibody staining. The Click-it reagent intercalates as a fluorescent nucleotide into the replicating DNA strand, marking the cells that are proliferating. The blocking buffer was then aspirated, and the primary antibody was added. The samples were stained with rabbit monoclonal anti-E-cadherin (E-cad;Rb, mAb, Cell Signaling) at 1:500 in blocking buffer for 12 hours at 4ºC on a rocker. They were then triple rinsed with 1x PBS, and the secondary antibody was added. Goat-anti-rabbit Dylight 488 (Thermo Scientific) was used at 1:1000 in blocking buffer. The secondary antibody was aspirated, and 500ng/ml DAPI was added to each channel. Samples were incubated at room temperature for 1 hour and were triple rinsed with 1x PBS. Blocking buffer was added to each sample to ensure hydration during any storage periods.

The whole organ and single lobe samples were cleared before imaging: first they were dehydrated in 100% Methanol baths for 5 minutes, repeated 3 times. The samples were then placed in a 1:1 Benzyl Alcohol to Benzo Benzoate solution (BABB) for 3x15 minute incubation periods. The samples were stored and imaged in BABB. They were imaged within a day of clearing using a Zeiss epifluorescent microscope and a Zeiss single photon confocal microscope.

2.2 Single Lobe Culture Model

The model was created by suturing off postnatal day 7 (p7) murine prostate ventral lobe explants and securing the two threads of the suture between two PDMS well walls in order to suspend the lobe in explant culture media. This was done in order to control the degree of external hydrostatic pressure, as well as to prevent the lobe from experiencing increased shear stress or tension in membrane culture. If the lobes were cultured on a membrane or stiff surface, the mesenchymal cells differentiate into myofibroblast and move away from the luminal structure, destroying the integrity of the lobe. The lobes of my model were explanted at age p7 because that is both when lumen growth is high, smooth muscle is beginning to differentiate, and the lobe is small enough for whole-lobe microscopy. The control sample was suspended in explant media and cultured for 36 hours in an incubator at 37ºC. To simulate an increased external pressure and simulate a fibrotic environment similar to that found in BPH, lobes were cultured in 80% Growth Factor Reduced Matrigel-Media. To simulate an increase in intraluminal pressure, 1uM solution of Forskolin was added to the media. The Forskolin increases cAMP production and stimulation of the PKA pathway, increasing sodium channel transport to the apical side of the epithelium as well as increasing sodium channel function[31]. This increases sodium transport and subsequently water transport into the lumen, increasing intralumenal pressure.

2.2.1 Single Lobe Dissection

Prior to dissection, suture threads were tied into loose individual knots in preparation. The initial technique mentioned in **section 2.1.1**. was followed. After removal of excess tissue, the bladder was cut off to more readily expose the ventral

lobes. A suture knot could then be used to tease apart the naturally bifurcated ventral lobe. The suture was then slipped over one lobe, and tightened, sealing off that lobe. Left and Right lobes were noted. Once the second lobe was secured via suture knot as well, forceps were used to peal the urethral tissue away, dislocating both tied ventral lobes away from the remaining tissue. Only the ventral lobes were used in this model because the murine ventral lobe is most comparable in structure and function to the human prostate. Therefore, multiple cell types and structures remained while external variables such as membrane stiffness, nutrient transport, and consistent hydration were mitigated.

2.2.2 Suture Suspension Device Construction

Forty gram 9mm wells of PDMS were used to create wells at 2mm thickness. The PDMS was cut into 3cm by 3cm squares and was cored with 1.5cm circular device. The squares were then soaked in 70% ethanol for minimum for 5min. Once square was placed in a well of a sterile 6 well tissue culture dish. Then, using forceps to hold the excess ends of the knots, the explant was placed across the circular hole and was suspended by draping the excess suture ends across either side of the PDMS "well." A second PDMS "well" was then placed on top of the initial to secure the suture ends in place, keeping the explant suspended, and allowing for media to cover the explant.

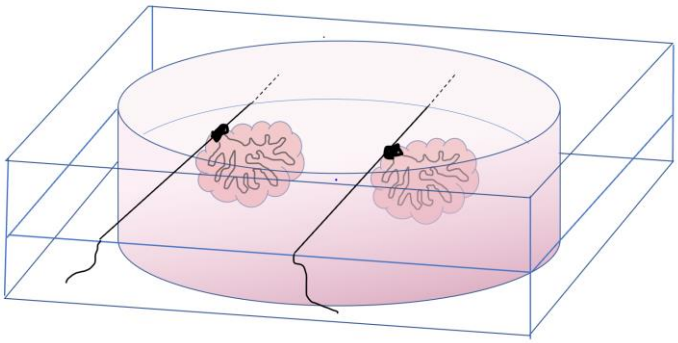

Figure 5; Diagram of Suture Suspension Device described above.

Microscopy methods mentioned in **section 2.1.3** were used when staining and imaging the tissues. The explants were co-stained with E-cadeherin to identify the epithelial structures, Edu to identify proliferation, and DAPI as a nuclear stain. Proliferating epithelial cells were identified by co-expression of E-cadherin, DAPI and EdU, whereas proliferating mesenchymal cells were identified by the duel expression of DAPI and EdU.

2.3 Mesenchyme Free Organoid Model

Primary prostate epithelial cells were isolated manually, macerated to separate cell clumps, and cultured in a 1mm thick layer of 8:2 Growth Factor Free Matrigel in epithelial explant media. The cells and Matrigel were then covered in 500uL of epithelial explant media, a media with a mixture of epithelial growth factors and Rho-associated protein kinase (ROCK) inhibitor to prevent the primary epithelial cells from going through EMT or differentiating into myofibroblasts in the Matrigel. The ROCK inhibitor specifically allowed for an increase in actin bundling and increased likelihood of epithelial colony formation[32]. The cells cultured for about 1.5 weeks before clear, hollow luminal spheroids formed.

2.3.1 Primary Epithelium Manual Isolation

The dissection process described in **section 2.1.1.** was adapted to adult CD1 mice, as the adult mice had larger prostates and therefore more epithelium. The bladder was cut away to expose the ventral lobes. The two proximal lumen of the ventral lobes could then be identified and used as point from which to pull the lobes away from the urethra with a sharp dissecting forceps. Once separated, the lobes were placed in a well of 10% protease in DI water for 15 minutes to degrade the mesenchymal integrity and loosen the mesenchyme attachment to the epithelial layer of the lumen. The lobes were then rinsed with 100% Fetal Bovine Serum to inhibit further proteolytic action on the tissue. The dissection was then continued in explant media rather than 1x PBS in a 9mm dish in which the bottom was coated in a thin layer of polymerized PDMS. The following dissection technique takes between one to two hours, so explant media was used to increase cell survival during the procedure. The bottom of the dish was coated in PDMS to prevent possible damage to dissection tools while holding the cell layers in place. Forceps can be used to initially pull away a large portion of the distal mesenchyme. Once removed, the proximal end of the lumen of a lobe was secured with forceps while fine tungsten needles were used to scrape away the remaining mesenchymal cells along each individual branch. Care must be taken to maintain the luminal structure, as this makes it easier to transport the epithelium to a fresh dish of epithelial explant media until all epithelium is clear. Using a dulled Tungsten needle and forceps, the cleared epithelial branches were macerated to separate and suspend the cells in the surrounding media. The media can then be pipetted and combined 2:8 parts with Growth Factor Free Matrigel and plated. The Matrigel mixture was incubate at 37^{o}C for 20 minutes to solidify, then add 300uL of room temperature epithelial explant media to the well to keep the gel hydrated.

Epithelial integrity was confirmed by assessing cell shape, lack of migration within the gel, and E-cadherin (ECAD) antibody staining.

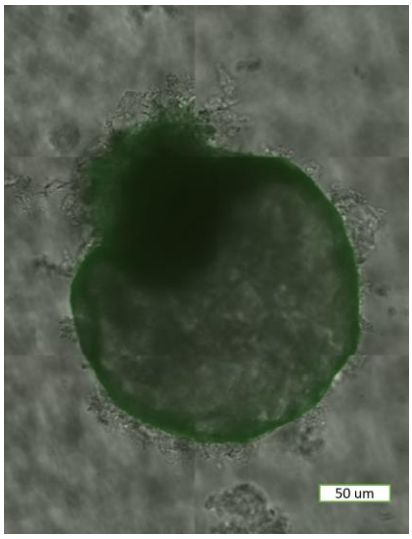

Figure 6; Brightfield overlay of ECAD (green fluorescent antibody stain) image of a primary epithelial spheroid cultured for two weeks.

Table 1: Epithelial Explant Media Preparation: Reagents and their percent total solution

Reagents	**% of Total Solution**
DMEM F12	94%
5µg/mL EGF	0.10%
L-Glutamine	1.00%
Heat-inactivated, Charcoal-stripped FBS	5%
Penn/Strep	1.00%
5 mM ROCK inhibitor Y-27632	0.20%
100 nM DHT	1%
Matrigel	5%

2.4 Intubation Suspension Model

This model was made as an alternate to the single lobe suspension model. A two well system was created out of PDMS and connected by a pulled glass capillary with one dull end in one well and one sharp end in the other. The well height could vary by adding plasma cleaned PDMS cutout wells to either of the wells of the connected two well base. This allows for a more drastic manipulation of hydrostatic pressure on either the well in which the explant will be suspended (external pressure) or the well from with the explant is intubated (internal pressure).

2.4.1 Intubation Technique

The dissection technique used in **section 2.1.1.** was used. Once the excess tissue was removed from the bladder, prostate, and urethral system, a loose suture knot was slipped over the urethra. The forceps were used to gently grasp a caudal end of the urethra and slide the pulled needle down the center shaft through. Care was taken not to let the needle slide between the skin and the tighter smooth muscle layer rather than down the tighter urethra. One pair of forceps was used to keep the explant from slipping off, while the second was used to slide the suture knot down the urethra and tighten it to secure the urethra onto the capillary. Once tightened, the two suture ends were shoved into the adjacent PDMS sides using the forceps, keeping the ends taught. Both wells are filled with a minimum of 500uL of explant media.

2.4.2 Intubation Device Construction

40 gram 90mm dishes were filled with PDMS to be about 20mm thick. Once polymerized, the PDMS was cut into 25mm by 70mm rectangles and two 15mm diameter circular cutouts were made adjacent to each other within the rectangle. Glass capillaries (OD/ID = 150μm/87μm) were pulled to form sealed micropipettes for

prostate intubation. A 150μm diameter punch was pushed laterally the center barrier between the two wells to create a slight opening. The pulled capillary was then pushed dull end first through the opening to connect the two wells. The PDMS with capillary was then plasma cleaned and adhered to a 40mm by 80mm glass coverslip. This forms the base of the device. If intending to increase hydrostatic pressure to one side once the organ is intubated, a square PDMS well with a 15mm diameter cutout can be plasma cleaned and adhered over the desired well.

Chapter 3

RESULTS

3.1 Explant Model Development

Several types of explant models were created for varying purposes. The first whole organ explant model was successfully used to identify a phenotypic difference in prostate survival and morphology in a closed system (sutured) vs an open system (unsutured). This model was only used for qualitative study.

3.1.1 Whole Prostate and Urethra Explant Culture

Whole prostates were successfully dissected and cultured for 48 hours on the membrane suspended device shown in Figure 3. A Live/Dead assay was used to validate the survival of cells and lack of internal necrosis during culture. An EdU kit by Thermo Fisher was used to label actively replicating cells during the exposure pulse of Thermo Fisher's "reagent A," and after fixation, a click chemistry reaction fluorescently tagged the labeled cells with Alexafluor 647. The closed culture system prostate explants have significantly more EdU labeled epithelial cells, particularly in the ventral lobes, as opposed to the open culture system explants.

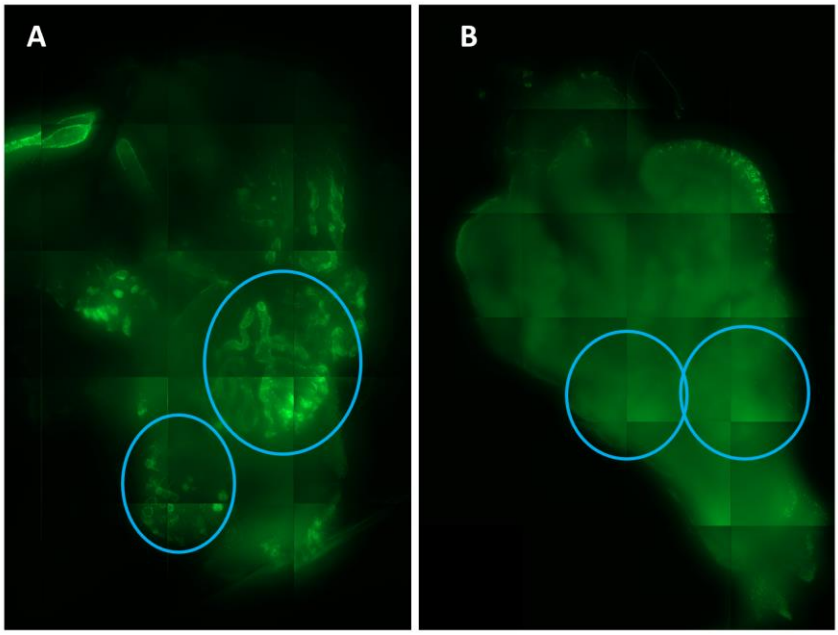

Figure 7; Difference in ventral lobe luminal proliferation during two days of culture in the membrane suspended device between A) sutured whole prostate-urethra explant and B) unsutured whole prostate-urethra explant. Proliferating cells were labeled in culture using an EdU kit for a 7 hour pulse, and is labeled via increased green fluorescence. The blue circles highlight the location of the ventral lobes for comparison.

After fixation, antibody staining was used to label ECAD, an epithelial cell marker. A staining technique was successfully optimized and can be used to fluorescently define the luminal structures. Red and Green autofluorescence are present in all images of the tissue as seen in Figures 6 and 7. Though less obvious than the difference in proliferation described above, the morphology of lumen in closed culture system explants varies from that of open system explants. Though pushed slightly upward due to suture placement and imaging angle, the ventral lobes of the

closed explant are more bulbous and further developed with more distal buds than the lobes of the open system.

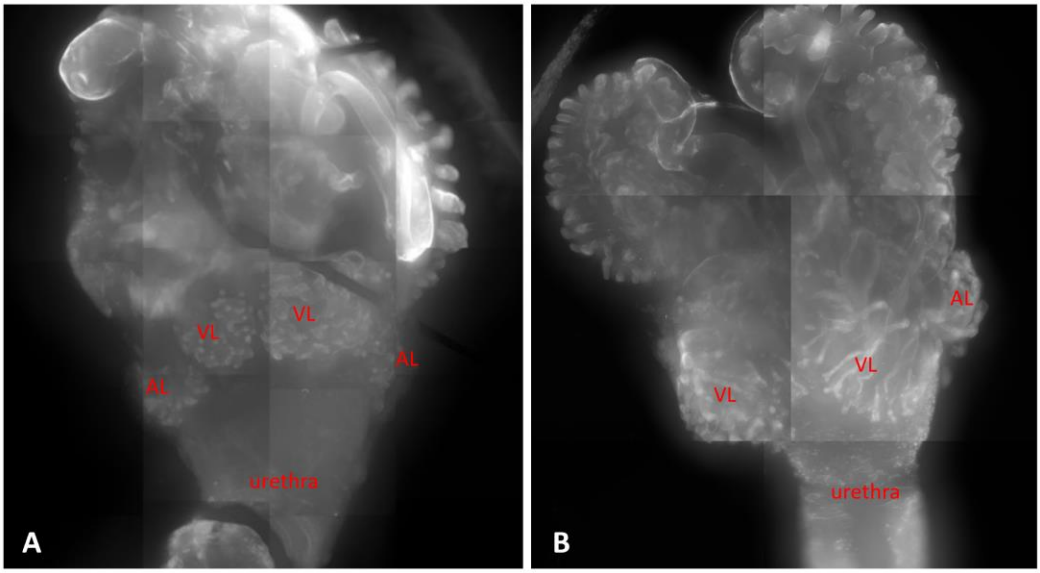

Figure 8; Maximum projection of fluorescently labeled ECAD (white) showing morphological differences in the lumen morphology – especially the ventral lobes – in A) a sutured prostate system and B) an unsutured prostate system after two days of culture membrane suspended culture. VL stands for ventral lobe, AL stands for anterior lobe

3.1.2 Single Ventral Lobe Culture

Both ventral lobes were successfully dissected, sealed at the proximal lumen with a suture, and suspended in media without encountering stiff surfaces for 36-48hour culture. Mechanical forces were manipulated using four different conditions with explant media as the control. Intralumenal pressure was increased using 1μM Forskolin in explant media, resulting in overall increased proliferation, and generally resulted in the largest lobe volumes. Environmental stiffness (to simulate fibrosis) was simulated using 4:1 Matrigel in explant media which resulted in variable epithelial

proliferation and a mild increase in mesenchymal proliferation. The final condition consisted of a 1uM Forskolin treatment of the 4:1 Matrigel in explant media which resulted in a significant increase in epithelial proliferation and a relative decrease in mesenchymal proliferation. Cells were counted every 50μm through the z-plane of the confocal images. A one-way A-Nova test was used to assess significance of epithelial cells proliferating.

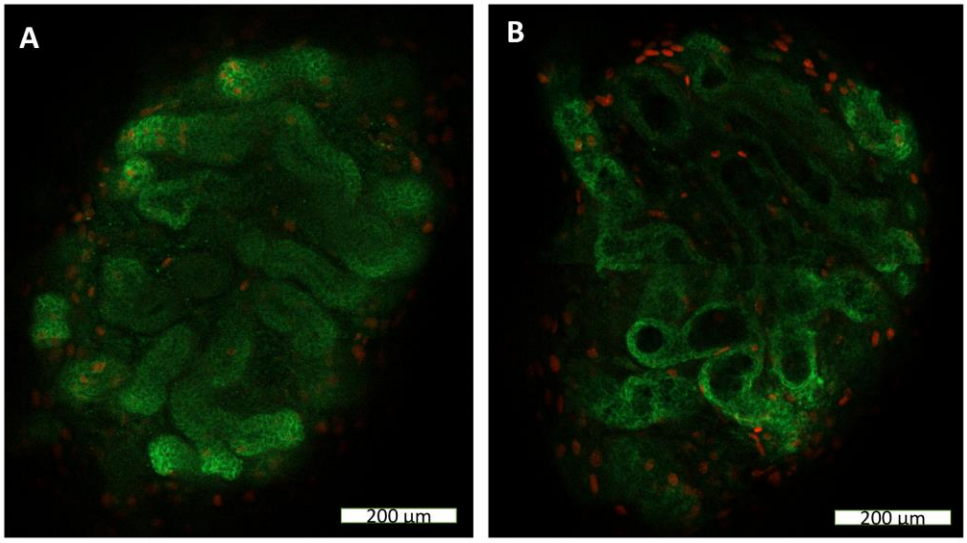

Figure 9; The same z-slice of two samples highlighting the different ECAD organization in two ventral lobe samples, A) sample cultured in explant media so opposed to B) sample cultured Matrigel and Forskolin. ECAD is fluorescently labeled green, EdU labeled cells are red.

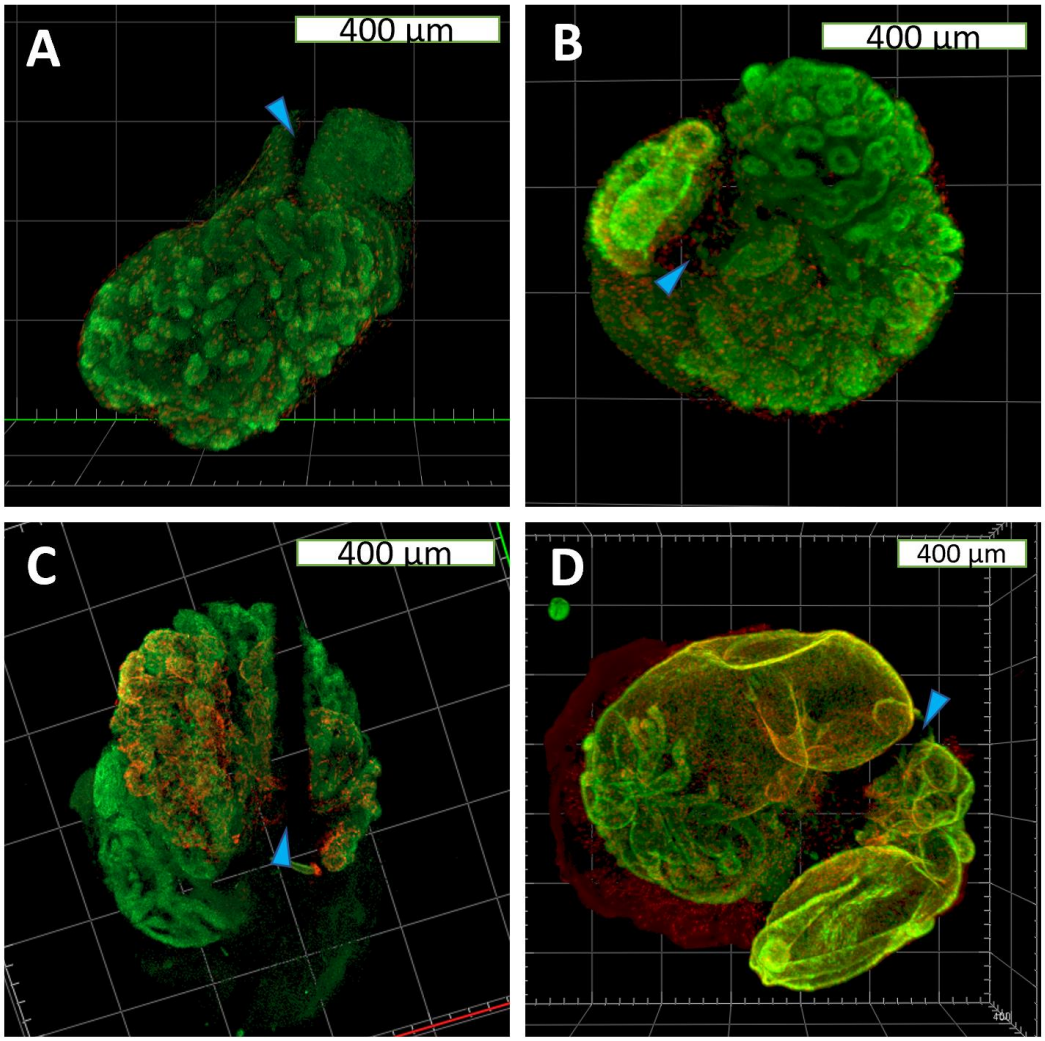

Figure 10; Immunofluorescent confocal images of ECAD expression (green) and 5 hour EdU labeling (red) in ventral lobes cultured for 48 hours with A) explant media, B) 4:1 Matrigel in explant media, C) 4:1 Matrigel in media treated with 1uM Forskolin, and D) explant media with 1uM Forskolin. The blue arrows define the suture in the image.

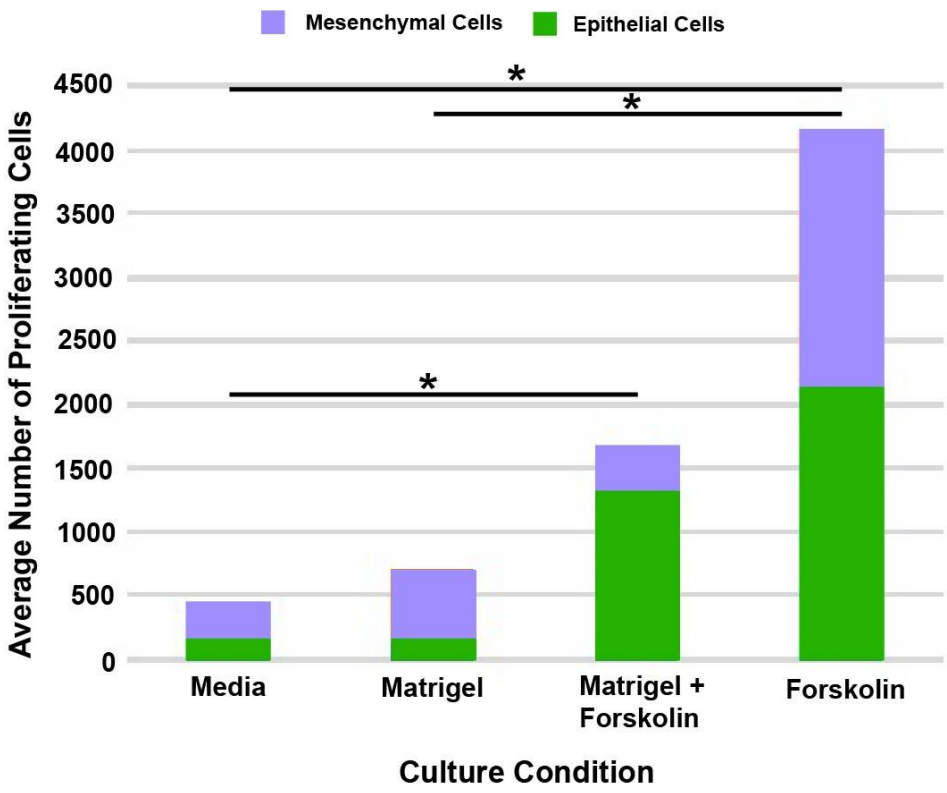

Figure 11; Graph depicting average number of ventral lobe epithelial and mesenchymal cells proliferating during a 7 hour pulse. Four main culture conditions were used as described above.

3.1.3 Mesenchyme Free Epithelium Spheroid Culture Model

A culture model of isolated primary epithelial cells was successfully created. The spheroids are embedded in 4:1Matrigel in epithelial explant media that is pipetted onto a thin base coating of 100% Matrigel. Once gelled, 200-500 μL of epithelial explant media is pipetted on top, keeping the gels hydrated in culture. Initially the cells tend to group in small clusters. Over the first 4- days they form solid spheres, and slowly dissolve the interior cells over the next 5 days. After about 10 days of culture, hollow luminal spheroids have formed. If left longer than 15 days, the spheroids begin to elongate and lose shape. It is worth mentioning that epithelial cells isolated from

postnatal mice never successfully formed spheroids and much more readily differentiated into myofibroblasts or lysed. Epithelial cells isolated from adult mice, did form spheroids when embedded and only differentiated if they came into contact with a stiff surface.

The epithelial spheroids were immunofluorescently stained for ECAD and smooth muscle myosin (SMM). The spheroids expressed ECAD, suggesting the cells retained their epithelial phenotype, and they did not express smooth muscle myosin, a protein expressed by the myofibroblast-like cells that can differentiate from isolated primary epithelium.

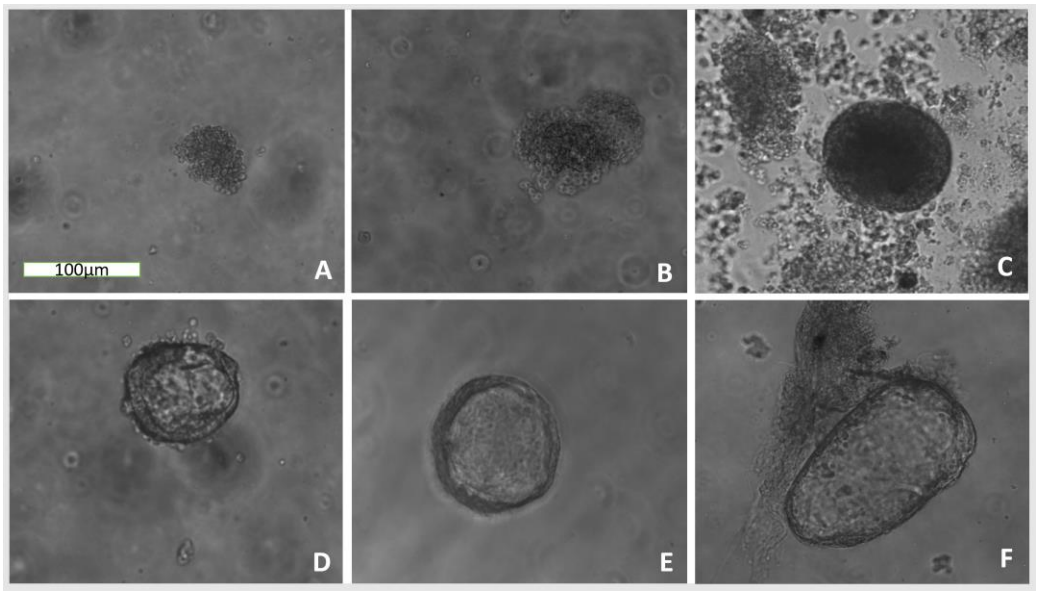

Figure 10; A series of images taken of primary epithelial cells in their various stages of development into spheroids. A) was taken at 24 hours after embedding, B) taken at 2 days after embedding, C) taken at 5 days, D) taken at 8, days, E) taken at 10 days, and F) taken at 16 days.

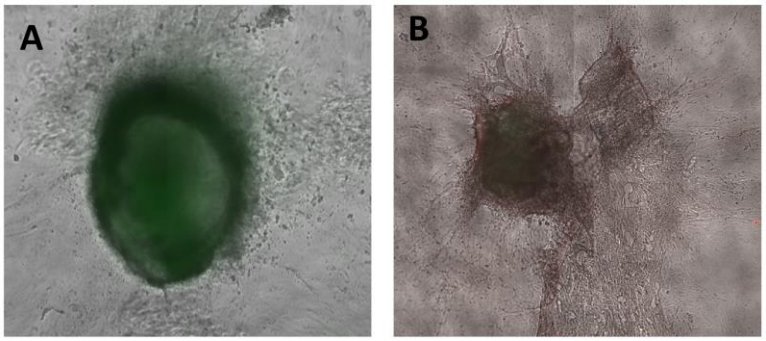

Figure 11; Spheroids immunofluorescently stained for ECAD and SMM. A) an epithelial spheroid expressing ECAD but not SMM compared to B) a spheroid losing ECAD expressing, while expressing SMM as the cells differentiate towards myofibroblasts.

Chapter 4

DISCUSSION

4.1 Comparing Models

Four models total were constructed to observe the effect of mechanical forces on prostate luminal development. Two, the whole organ explant and the single lobe culture model, were analyzed via immunofluorescent staining and microscopy. The third, spheroid culture, was validated using immunofluorescent microscopy as well, and preliminary data has been collected measuring the pressure maintained within the spheroid. The final model was created to mitigate variables introduced by chemical manipulation of pressure in the single lobe culture model, however, data has not been collected using this model yet.

4.1.1 Whole Organ Explant Model

The whole organ explant mode was created with the intention to visualize the luminal morphology of the murine prostate and create a simple pressure versus no pressure prostate system to identify any initial change in the tissue due to mechanical forces. Imaging explants at various ages showed that the ventral lobes grow asymmetrically and systematically. After initial budding from the urethra around embryonic day 20, the lumen develops into a hand-like branching structure by postnatal day 4, maintaining the main proximal lumen (connected to the urethra). By postnatal day 6 smooth muscle is differentiating along the branching epithelium[10,15], and as the lobe develops, the distal branching becomes more complex, eventually even intertwining by adulthood. Therefore, typical analytical measures for organ maturity such as branch number or distal bud count cannot be applied to assess stage of prostate development. This makes immunofluorescent imaging of an entire luminal structure

important to establish spatial relativity for any analytical measures applied as the organ developed. Postnatal days 5 and 7 were used for explant culture because by p5, ventral lobe branching is significant and stroma is developing, allowing for epithelial-smooth muscle-mesenchyme interactions to be included in the model. Additionally, it is significantly easier to accurately sex postnatal mice at p7. Unfortunately, the total thickness (z-plane) of the dorsal prostate, urethra, and ventral lobe is too large to accurately image at more than 10x magnification using an epifluorescent or single photon confocal microscope. To maintain continuity between samples, the explants were all imaged with the ventral side against the coverslip.

There was an observable difference in prostate morphology and proliferation in closed (sutured) vs open (unsutured) prostate systems. Generally, the sutured prostates exhibited fuller, more robust and complex luminal morphology than the unsutured prostates. The unsutured prostates had a tendency to appear withered with less luminal development and lower general volume. To more specifically determine the proliferative difference between the sutured and unsutured samples, a Thermo Fisher EdU kit was used. Multiple pulse times were tried, and a pulse of 7 hours was determined the most informative, as it accounted for the relatively slow proliferative rate of postnatal tissue compared to embryonic tissue or generic cell lines. The sutured prostate showed significantly more proliferation than the unsutured. Exact quantification (via cell counting or fluorescent intensity) was not possible due to the thickness of the tissue and the inability for the light to penetrate at a consistent intensity through entire the sample.

This difference in proliferation (and the fact it is mostly localized along luminal structures) is suggestive of a mechanosensitive pathway inducing epithelial

growth. Literature has shown that hypotonic stress induces ATP release and activates the MAPK and p13k pathways, subsequently activating downstream transcription factors that lead to increased proliferation[6].

Additionally, two logistical problems presented themselves with the membrane culture. If the explant and device were completely submerged to prevent accidental dehydration in the incubator, about 40% of the samples would pop off the membrane. This was mitigated, by applying a large media droplet over the explant (rather than submerging it) to keep it on the membrane using surface tension – this however, increased the likelihood of accidental dehydration. Culturing the explant against a membrane also meant culturing the explant against a surface stiffer than the physiological environment. If cultured for more than 24 hours, the mesenchymal cells began to migrate along the membrane, decreasing organ integrity. Subsequently, the single lobe culture model was created to combat some of these limitations.

4.1.2 Single Lobe Culture Model

The single lobe model looks only at the ventral lobe. Though the detail of the procedure increases the likelihood of human mistake during dissection, the lobes are usually less than 500μm thick, allowing for significantly better penetration of the microscope laser. Therefore, analysis via cell counting is possible.

The effect of the Forskolin treatment was notable. Forskolin was used because it has been known to increase ion channel activity, subsequently increasing the movement of water into the luminal space and increasing luminal hydrostatic pressure. However, Forskolin is also notorious for its ability to activate adenylyl cyclase, increasing overall cAMP production, which can increase a variety of cellular functions such as increasing metabolism, prostaglandin activity in smooth muscle, and indirectly

activating downstream transcription factors – all of which are possible confounding variables. Therefore, the drastically increased proliferation, especially that of the mesenchyme, could be due to increased cAMP second messenger activity. The drastic luminal swelling and respective epithelial proliferation, however, are more likely due to the increased hydrostatic pressure, supporting the hypothesis that the epithelium is reactive to fluid-induced mechanical forces.

Interestingly, the Matrigel and Forskolin cultures show more epithelial proliferation in comparison to mesenchymal proliferation. This could support the idea that mesenchymal proliferation is regulated by environmental stiffness. Furthermore, it is possible that the "external resistance" provided by the Matrigel and nonproliferative mesenchyme against the increased internal hydrostatic pressure, compresses the epithelium. This would suggest that compression leads to increased epithelial proliferation (likely decreased mesenchymal proliferation as well) with conserved morphological regulation.

The Matrigel culture showed no significant difference in epithelial proliferation compared to the explant media control culture. This suggests that the environmental resistance provided by Matrigel did not reduce mesenchymal proliferation alone, nor did it enhance epithelial proliferation in the Matrigel and Forskolin experiment.

It is also worth mentioning that the ECAD organization varies between control samples and those cultured in Matrigel and Forskolin. As shown in Figure 7, the control ECAD is ordered, outlining epithelial cells of consistent size and shape along the lumen. In the Matrigel and Forskolin culture, the ECAD expression is more irregular – the cells are nondescript shapes, all varying in size, suggesting the ECM

and junctional skeletal protein expression could be altered in response to the compression[12,18]. Additionally, the lumen of the Matrigel and Forskolin samples seems to have more irregularities in their diameter compared to the lumen of the control. Rather than one relatively congruent tube, the Matrigel and Forskolin samples are more prone to "blebbing" in random areas long the branches, a morphology somewhat comparable to the irregular lumen shapes and epithelial ingrowths found in pathological PIN structures. It is possible that the Matrigel and Forskolin model mimic a cancerous microenvironment, implicating compression as a possible factor in pathological epithelial growth.

4.2 Future Directions

Because chemical manipulation provides so many compounding variables, I have created an intubation system in which one is able to manually manipulate intraluminal pressure. By changing fluid volume in one well, one can increase pressure experienced in the connected well. For example, if the media is increased in the left well, fluid would want to flow through the connecting capillary which would be fixed in the urethra of the closed prostate system in the right well. Therefore, the pressure inside the prostate system would increase proportionally to the volume of fluid added. Using Amira imaging program, I have calculated the average total volume of the p7 prostate lumen, so the theoretical pressure increase within the prostate can be calculated. The external hydrostatic pressure experienced by the explant can be manipulated by increasing volume in opposite well.

The spheroid model was created to quantify the change in intraluminal pressure created by various chemical manipulators. The capabilities of our lab have made taking baseline spheroid pressures and spheroid pressure when exposed to

Forskolin possible, however how the data are preliminary and not included in this paper. It could also be used as a way of investigating solely epithelial responses to changes in fluid induced forces, eliminating the confounding variables of stromal and mesenchymal crosstalk[17].

Chapter 5

CONCLUSION AND FUTURE DIRECTIONS

Benign prostate hyperplasia and prostate cancer are two of the most common diseases faced by men, and both diseases involve abnormal epithelial expression and growth. As more and more mechanically active ion channels are being discovered and identified in the prostate, it is increasingly likely that fluid induced mechanical forces play are large role in development as well as pathology progression. This study poses to first create a physiologically relevant, 3D culture model of the growing prostate which can then be used to confirm that mechanical forces influence the luminal development and morphology of the prostate.

Four different models were created to elucidate the role of fluid induced forces, the first of which entailed suspending the entire organ on a membrane in culture, the second focused only on ventral lobe culture, the third on primary epithelial spheroids, and the fourth involves intubation of the urethral to manually alter intralumenal pressure. The results showed that morphology of the prostate does change when cultured as either a closed system or open system, with increased luminal volume and proliferation in a closed system compared to open. Further studies focused on the ventral lobe showed that unsurprisingly, Forskolin significantly increases proliferation of both the mesenchyme and epithelium. However, lobes cultured in Matrigel and treated with Forskolin showed only significant epithelial proliferation. Because lobes cultured in Matrigel alone showed no significant change in proliferation than lobes cultured in explant media (the control), this suggests that the resistance provided by the Matrigel combined with the increased hydrostatic pressure of the lumen might create a compressive environment that stimulates epithelial proliferation.

Future directions involve manually altering pressure using an intubation device to avoid the confounding variables introduced by chemical manipulation of luminal pressure. Additionally, primary epithelial spheroid cultures could be used to identify epithelial-specific reactions to changes in fluid induced forces. This would help determine whether the epithelium is influencing the stroma and mesenchyme in response to changes in fluid forces or vice versa.

The results from this project provide an exciting starting point for the elucidation of mechanically sensitive pathways in prostate epithelium and their relationship with epithelial growth, both normal and pathological. Understanding the influence of mechanical forces and the mechanosensitive pathways implicated in prostate development and morphological regulation can provide insight into treatment targets for BPH or new targets for prevention of prostate cancer.

REFERENCES

1. Lim, K. B. (2017). Epidemiology of clinical benign prostatic hyperplasia. *Asian Journal of Urology*, *4*(3), 148–151. https://doi.org/10.1016/j.ajur.2017.06.004

2. Dai, X., Fang, X., Ma, Y., & Xianyu, J. (2016). Benign Prostatic Hyperplasia and the Risk of Prostate Cancer and Bladder Cancer. Medicine, 95(18). https://doi.org/10.1097/MD.0000000000003493

3. Fibbi, B., Penna, G., Morelli, A., Adorini, L., & Maggi, M. (2010). Chronic inflammation in the pathogenesis of benign prostatic hyperplasia. International Journal of Andrology, 33(3), 475–488. https://doi.org/10.1111/j.1365-2605.2009.00972.x

4. Brawer, M. K. (2005). Prostatic Intraepithelial Neoplasia: An Overview. *Reviews in Urology*, *7*(Suppl 3), S11–S18.

5. Strand, D. W., & Goldstein, A. S. (2015). The many ways to make a luminal cell and a prostate cancer cell. *Endocrine-Related Cancer*, *22*(6), T187–T197. https://doi.org/10.1530/ERC-15-0195

6. Frontiers | Disruption of Prostate Epithelial Differentiation Pathways and Prostate Cancer Development | Oncology. (n.d.). Retrieved January 9, 2019, from https://www.frontiersin.org/articles/10.3389/fonc.2013.00273/full

7. Loss of E-Cadherin Promotes Metastasis via Multiple Downstream Transcriptional Pathways | Cancer Research. (n.d.). Retrieved January 8, 2019, from http://cancerres.aacrjournals.org/content/68/10/3645.short

8. Chen, P., Yin, J., Guo, Y., Xiao, H., Wang, X., DiSanto, M. E., & Zhang, X. (2018). The expression and functional activities of smooth muscle myosin and non-muscle myosin isoforms in rat prostate. *Journal of Cellular and Molecular Medicine*, *22*(1), 576–588. https://doi.org/10.1111/jcmm.13345

9. Marker, P. C., Donjacour, A. A., Dahiya, R., & Cunha, G. R. (2003). Hormonal, cellular, and molecular control of prostatic development. *Developmental Biology*, *253*(2), 165–174. https://doi.org/10.1016/S0012-1606(02)00031-3

10. Prins, G. S., & Putz, O. (2008). Molecular signaling pathways that regulate prostate gland development. *Differentiation; Research in Biological Diversity*, *76*(6), 641–659. https://doi.org/10.1111/j.1432-0436.2008.00277.x

11. Kügler, R., Mietens, A., Seidensticker, M., Tasch, S., Wagenlehner, F. M., Kaschtanow, A., … Middendorff, R. (2018). Novel imaging of the prostate reveals spontaneous gland contraction and excretory duct quiescence together with different drug effects. *The FASEB Journal*, *32*(3), 1130–1138. https://doi.org/10.1096/fj.201700430R

12. Maroto, R., Kurosky, A., & Hamill, O. P. (2012). Mechanosensitive Ca2+permeant cation channels in human prostate tumor cells. Channels, 6(4), 290–307. http://doi.org/10.4161/chan.21063

13. Wang, N., Dong, B.-J., Quan, Y., Chen, Q., Chu, M., Xu, J., … Gao, W.-Q. (2016). Regulation of Prostate Development and Benign Prostatic Hyperplasia by Autocrine Cholinergic Signaling via Maintaining the Epithelial Progenitor Cells in Proliferating Status. Stem Cell Reports, 6(5), 668–678. https://doi.org/10.1016/j.stemcr.2016.04.007

14. Kim, S.-Y., Yang, D., Myeong, J., Ha, K., Kim, S.-H., Park, E.-J., … So, I. (2013). Regulation of calcium influx and signaling pathway in cancer cells via TRPV6–Numb1 interaction. *Cell Calcium*, *53*(2), 102–111. https://doi.org/10.1016/j.ceca.2012.10.005

15. Down-regulated CFTR During Aging Contributes to Benign Prostatic Hyperplasia - Xie - 2015 - Journal of Cellular Physiology - Wiley Online Library. (n.d.). Retrieved December 15, 2018, from https://onlinelibrary.wiley.com/doi/abs/10.1002/jcp.24921

16. Thebault, S., Flourakis, M., Vanoverberghe, K., Vandermoere, F., Roudbaraki, M., Lehen'kyi, V., … Prevarskaya, N. (2006). Differential role of transient receptor potential channels in Ca2+ entry and proliferation of prostate cancer epithelial cells. *Cancer Research*, *66*(4), 2038–2047. https://doi.org/10.1158/0008-5472.CAN-05-0376

17. Asuthkar, S., Demirkhanyan, L., Mueting, S. R., Cohen, A., & Zakharian, E. (2016). High-throughput proteome analysis reveals targeted TRPM8 degradation in prostate cancer. *Oncotarget*, *8*(8), 12877–12890. https://doi.org/10.18632/oncotarget.14178

18. Kim, S.-Y., Yang, D., Myeong, J., Ha, K., Kim, S.-H., Park, E.-J., … So, I. (2013). Regulation of calcium influx and signaling pathway in cancer cells via TRPV6-Numb1 interaction. *Cell Calcium*, *53*(2), 102–111. https://doi.org/10.1016/j.ceca.2012.10.005

19. Nandigama, R., Padmasekar, M., Wartenberg, M., & Sauer, H. (2006). Feed Forward Cycle of Hypotonic Stress-induced ATP Release, Purinergic Receptor Activation, and Growth Stimulation of Prostate Cancer Cells. *Journal of Biological Chemistry*, *281*(9), 5686–5693. https://doi.org/10.1074/jbc.M510452200

20. Ferguson, D. R., Kennedy, I., & Burton, T. J. (1997). ATP is released from rabbit urinary bladder epithelial cells by hydrostatic pressure changes–possible sensory mechanism? *The Journal of Physiology*, *505*(2), 503–511. https://doi.org/10.1111/j.1469-7793.1997.503bb.x

21. Wadhera, P. (2013). An introduction to acinar pressures in BPH and prostate cancer. *Nature Reviews Urology*, *10*(6), 358–366. https://doi.org/10.1038/nrurol.2013.86

22. Gat, Y., Gornish, M., Heiblum, M., & Joshua, S. (2008). Reversal of benign prostate hyperplasia by selective occlusion of impaired venous drainage in the male reproductive system: novel mechanism, new treatment. *Andrologia*, *40*(5), 273–281. https://doi.org/10.1111/j.1439-0272.2008.00883.x

23. Regulation of Smooth Muscle Contraction by the Epithelium: Role of Prostaglandins | Physiology. (n.d.). Retrieved January 18, 2019, from https://www.physiology.org/doi/full/10.1152/physiol.00036.2010

24. Farfariello, V., Iamshanova, O., Germain, E., Fliniaux, I., & Prevarskaya, N. (2015). Calcium homeostasis in cancer: A focus on senescence. *Biochimica Et Biophysica Acta*, *1853*(9), 1974–1979. https://doi.org/10.1016/j.bbamcr.2015.03.005

25. Wang, W., Wang, L., Mizokami, A., Shi, J., Zou, C., Dai, J., … Zhang, J. (2017). Down-regulation of E-cadherin enhances prostate cancer chemoresistance via Notch signaling. *Chinese Journal of Cancer*, *36*. https://doi.org/10.1186/s40880-017-0203-x

26. Pearson, H. B., Phesse, T. J., & Clarke, A. R. (2009). K-ras and Wnt Signaling Synergize to Accelerate Prostate Tumorigenesis in the Mouse. *Cancer Research*, *69*(1), 94–101. https://doi.org/10.1158/0008-5472.CAN-08-2895

27. Damodarasamy, M., Vernon, R. B., Chan, C. K., Plymate, S. R., Wight, T. N., & Reed, M. J. (2015). Hyaluronan in aged collagen matrix increases prostate epithelial cell proliferation. *In Vitro Cellular & Developmental Biology. Animal*, *51*(1), 50–58. https://doi.org/10.1007/s11626-014-9800-z

28. Pećina-Šlaus, N. (2003). Tumor suppressor gene E-cadherin and its role in normal and malignant cells. *Cancer Cell International*, *3*, 17. https://doi.org/10.1186/1475-2867-3-17

29. Harvey, H. (1995). A unifying hypothesis that links benign prostatic hyperplasia and prostatic intraepithelial neoplasia with prostate cancer. Invited comments. *Pathology, Research and Practice*, *191*(9), 924–934. https://doi.org/10.1016/S0344-0338(11)80978-7

30. Miyazawa, K., Tanaka, T., Nakai, D., Morita, N., & Suzuki, K. (2014). Immunohistochemical expression of four different stem cell markers in prostate cancer: High expression of NANOG in conjunction with hypoxia-inducible factor-1?, expression is involved in prostate epithelial malignancy. Oncology Letters, 8, 985–992. https://doi.org/10.3892/ol.2014.2274

31. Woollhead, A. M., & Baines, D. L. (2006). Forskolin-induced Cell Shrinkage and Apical Translocation of Functional Enhanced Green Fluorescent Protein-Human αENaC in H441 Lung Epithelial Cell Monolayers. *Journal of Biological Chemistry*, *281*(8), 5158–5168. https://doi.org/10.1074/jbc.M509947200

32. Maldonado, M., Luu, R. J., Ramos, M. E. P., & Nam, J. (2016). ROCK inhibitor primes human induced pluripotent stem cells to selectively differentiate towards mesendodermal lineage via epithelial-mesenchymal transition-like modulation. *Stem Cell Research*, *17*(2), 222–227. https://doi.org/10.1016/j.scr.2016.07.009